Masses and β-Decay Spectroscopy of Neutron-Rich Odd-Odd ^{160,162}Eu Nuclei: Evidence for a Subshell Gap with Large Deformation at $N = 98$

D. J. Hartley,[1] F. G. Kondev,[2] R. Orford,[2,3] J. A. Clark,[2,4] G. Savard,[2,5] A. D. Ayangeakaa,[2,*] S. Bottoni,[2,†] F. Buchinger,[3] M. T. Burkey,[2,5] M. P. Carpenter,[2] P. Copp,[2,6] D. A. Gorelov,[2,4] K. Hicks,[1] C. R. Hoffman,[2] C. Hu,[7] R. V. F. Janssens,[2,‡] J. W. Klimes,[2] T. Lauritsen,[2] J. Sethi,[2,8] D. Seweryniak,[2] K. S. Sharma,[9] H. Zhang,[7] S. Zhu,[2] and Y. Zhu[7]

[1]*Department of Physics, U.S. Naval Academy, Annapolis, Maryland 21402, USA*
[2]*Physics Division, Argonne National Laboratory, Argonne, Illinois 60439, USA*
[3]*Department of Physics, McGill University, Montréal, Québec H3A 2T8, Canada*
[4]*Department of Physics and Astronomy, University of Manitoba, Winnipeg, Manitoba R3T 2N2, Canada*
[5]*Department of Physics, University of Chicago, Chicago, Illinois 60637, USA*
[6]*Department of Physics, University of Massachusetts-Lowell, Lowell, Massachusetts 01854, USA*
[7]*Department of Physics, Zhejiang University, Hangzhou, China*
[8]*Department of Chemistry and Biochemistry, University of Maryland, College Park, Maryland 20742, USA*
[9]*University of Manitoba, Winnipeg, Manitoba R3T 2N2, Canada*

(Received 19 January 2018; revised manuscript received 27 March 2018; published 4 May 2018)

The structure of deformed neutron-rich nuclei in the rare-earth region is of significant interest for both the astrophysics and nuclear structure fields. At present, a complete explanation for the observed peak in the elemental abundances at $A \sim 160$ eludes astrophysicists, and models depend on accurate quantities, such as masses, lifetimes, and branching ratios of deformed neutron-rich nuclei in this region. Unusual nuclear structure effects are also observed, such as the unexpectedly low energies of the first 2^+ levels in some even-even nuclei at $N = 98$. In order to address these issues, mass and β-decay spectroscopy measurements of the $^{160}Eu_{97}$ and $^{162}Eu_{99}$ nuclei were performed at the Californium Rare Isotope Breeder Upgrade radioactive beam facility at Argonne National Laboratory. Evidence for a gap in the single-particle neutron energies at $N = 98$ and for large deformation ($\beta_2 \sim 0.3$) is discussed in relation to the unusual phenomena observed at this neutron number.

DOI: 10.1103/PhysRevLett.120.182502

One of the foundations of the nuclear shell model [1,2], which explains the presence of the magic numbers at Z or $N = 2$, 8, 20, 28, 50, and 82, is the existence of large energy gaps (or shell closures) in the single-particle spectra at these exact nucleon numbers. However, energy gaps are not only limited to spherical, magic nuclei. By including deformation in the shell model [3,4], it is possible to describe many properties of nonspherical nuclei. Indeed, shell closures have also been invoked in the single-particle spectra of deformed nuclei, as these can stabilize the nuclear shape at high deformation. This is the case for neutron-rich nuclei in the deformed, light rare-earth region ($Z \approx 58$–68, $A \approx 140$–170), where measurements of masses, half-lives, and decay properties are critically important to better understand rapid-neutron capture nucleosynthesis (r process). While there are many open questions concerning this process, one particular problem is the elucidation of the observed peak in the elemental r-process abundances at $A \sim 160$ [5–8], which is thought to be influenced by the structure of many deformed nuclei for which little or no experimental information exists. Understanding the origin of this peak may be one of the keys to correctly identify the astrophysical conditions for the r process [9,10]. In addition, some unusual nuclear phenomena have drawn attention to this region. In particular, an unexpected minimum in the first 2^+ energies at a neutron number away from midshell ($N = 104$) [11] may indicate a local maximum of deformation, possibly due to another subshell gap in the single-neutron spectrum.

In this Letter, we report on new mass and β-decay studies of neutron-rich odd-odd ^{160,162}Eu nuclei. For the first time, multiple β-decaying isomers were identified in both nuclei and their excitation energies, and decay properties were determined from the measured masses and $\beta - \gamma - \gamma$ spectroscopy studies, respectively. We present evidence for the existence of a deformed subshell gap at $N = 98$, contrary to the conclusions drawn from recent studies, where such a closure was suggested to occur at $N = 100$ [12–14]. This in turn explains the unusual behavior of the first 2^+ levels observed in several even-even $N = 98$ nuclei of this region.

The mass and β-decay spectroscopy experiments were both conducted in the low-energy experimental area of the Californium Rare Isotope Breeder Upgrade (CARIBU) facility [15], located at the ATLAS facility at Argonne

TABLE I. Measured frequency ratios and determined mass excess (ME) for the ground and isomeric states in ^{160}Eu and ^{162}Eu.

Ion	$^{84}Kr^{+}$ ν_c ratio	ME (keV)
$^{84}Kr^{+}$	1.0	−82 439.335 (4)[a]
$^{160}Eu^{2+}$	0.952 978 970 2 (58)	−63 493.4 (9)
$^{160m}Eu^{2+}$	0.952 979 565 4 (51)	−63 400.4 (8)
$^{162}Eu^{2+}$	0.964 926 876 6 (97)	−58 723.9 (15)
$^{162m}Eu^{2+}$	0.964 927 901 (12)	−58 563.7 (19)

[a]ME value for ^{84}Kr taken from Ref. [20].

National Laboratory. For the mass measurements, CARIBU beams of the desired mass-to-charge ratio were further purified at a resolving power in excess of $m/\Delta m \approx 100000$ by a multireflection time-of-flight mass separator [16] before being delivered to the Canadian penning trap mass spectrometer [17]. The phase-imaging ion-cyclotron-resonance technique [18] was used to directly measure the cyclotron frequencies (ν_c) of $^{160g,m}Eu^{2+}$, $^{162g,m}Eu^{2+}$, and $^{84}Kr^{+}$ ions by measuring the phase advance of the orbital motion of trapped ions during a period of excitation-free accumulation time as outlined in Ref. [19]. This technique enables fast high-resolution ν_c measurements and is capable of producing results with sub-keV mass precision. Masses were then determined relative to the measured ν_c of $^{84}Kr^{+}$ and the values are given in Table I. From the obtained new results, isomers in both ^{160}Eu and ^{162}Eu were established for the first time at excitation energies of 93.0 (12) and 160.2 (24) keV, respectively.

The nuclear structure properties of the ground and isomeric states in ^{160}Eu and ^{162}Eu were subsequently investigated through β-decay measurements. The CARIBU beams were directed onto a β-decay counting station [21] composed of the SATURN moving tape system, four scintillator detectors for β-particle detection, and the X-Array spectrometer, with four germanium clover detectors, and one low-energy photon spectrometer, for γ-ray detection. The signals from the γ-ray and β-particle counters were processed with a digital data acquisition system and written onto disk in an event-by-event mode. Given the previously known β-decay lifetimes of ^{160,162}Eu [22,23], tape-moving cycles of 180 s growth, 180 s decay time for ^{160}Eu and 50 s growth, 50 s decay time for ^{162}Eu, with 1 s for tape movement, and 4 s for background detection were selected in the present β-decay studies. In the off-line analysis, several matrices were generated, including β-particle gated E_γ-E_γ coincidence matrices that were used to construct the decay scheme of the ^{160}Gd and ^{162}Gd daughter nuclei, as well as β-particle gated E_γ-time histograms to deduce the half-lives of the observed β-decaying states.

Examples of β-particle gated $\gamma-\gamma$ coincidence spectra are presented in Figs. 1(a) and 1(b). It can be seen that in ^{160}Gd and ^{162}Gd the ground-state bands are populated up to

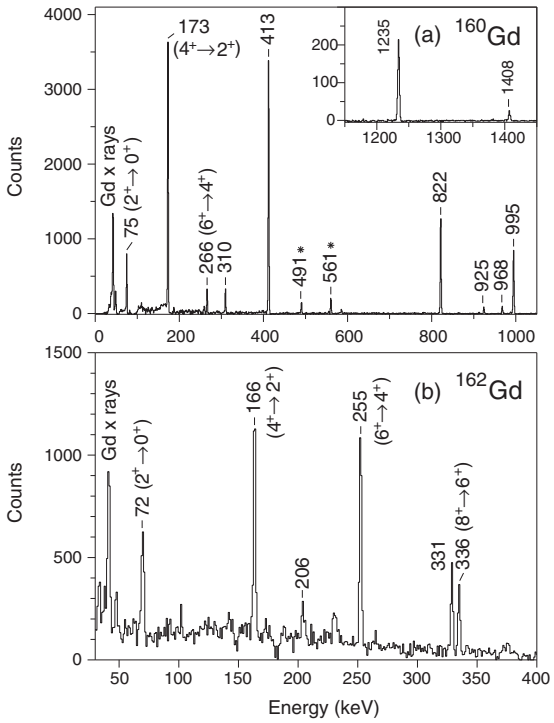

FIG. 1. (a) Spectrum of ^{160}Gd γ rays in coincidence with the 516-keV transition; the transitions labeled with a star feed the 1999-keV state. (Inset) Display of the high-energy lines from the same spectrum. (b) Summed spectrum resulting from coincidences with the 166- and 255-keV γ rays in the ground-state band of ^{162}Gd.

a spin of $I^\pi = 6^+$ and 8^+, respectively, thus implying that both ^{160}Eu and ^{162}Eu parent nuclides have a relatively high-spin β-decaying state.

Prior to the present Letter, the ^{160}Eu decay was studied in Refs. [24–27], where only a single low-spin β-decaying state with a half-life of $T_{1/2} = 38\,(4)$ s [22] was reported. In contrast, our data clearly indicate the presence of two β-decaying levels, one of high spin and the other of low spin. The former preferentially decays to the 1999-keV level of the daughter ^{160}Gd nuclide, shown in the decay scheme of Fig. 2. The observed depopulating transitions, coupled together with the previously known structure of ^{160}Gd [22], suggest spin and parity of $I^\pi = 4^+$, $5^\pm$, or 6^+ for this level. However, $I^\pi = (5^-)$ is preferred given the proposed configuration for the 1999-keV state, as discussed below. The strongest depopulating branch occurs via the 516-keV γ ray to the newly identified $I^\pi = 4^+$ state at 1483 keV. The spin and parity of this level are established by the observation of 1408-, 1235-, and 968-keV transitions to the $I^\pi = 2^+$, 4^+, and 6^+ members of the ground-state band, respectively. The transitions that follow the decay of the 1999-keV state exhibit similar half-lives and, after adding several time spectra together, a value of $T_{1/2} = 42.6\,(5)$ s was deduced for the high-spin β-decaying state of ^{160}Eu, as seen in Fig. 3(a). Transitions that were identified as only resulting

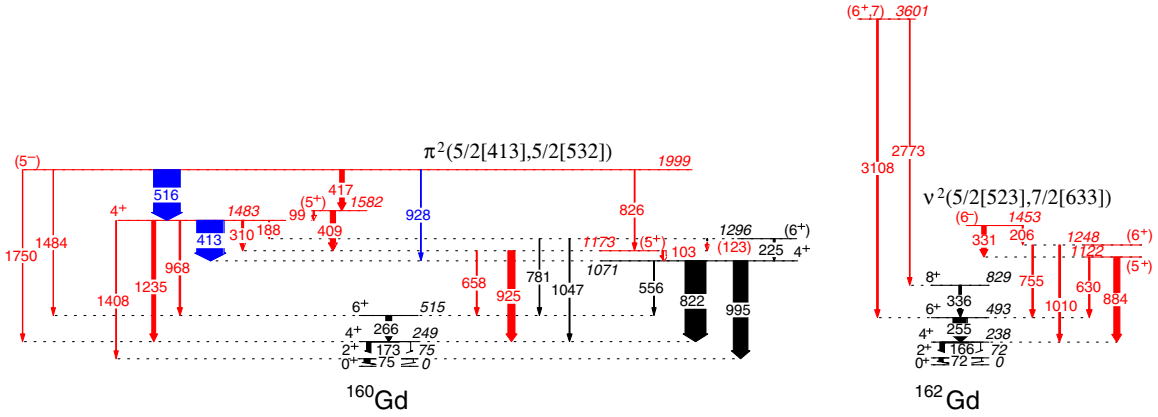

FIG. 2. Partial level schemes of ^{160}Gd (left) and ^{162}Gd (right) resulting from the β decay of the high-spin states in ^{160}Eu and ^{162}Eu, respectively. Previously known transitions are shown in black, new transitions are red, and reordered transitions are in blue.

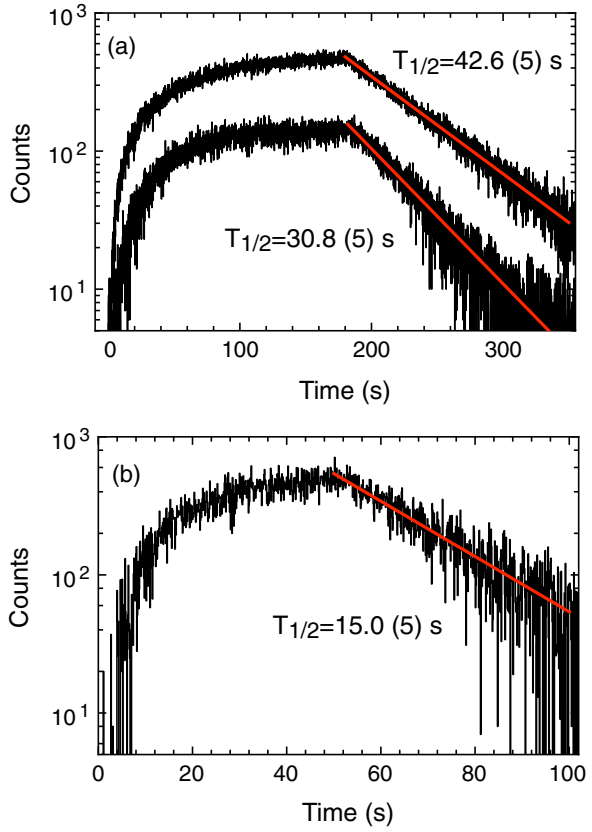

FIG. 3. (a) Summed background-subtracted time spectra from the two β-decaying states in ^{160}Eu. The 413-, 516-, 822-, and 995-keV γ rays, following the decay of the high-spin state in ^{160}Eu, were used to produce the top spectrum, while the 1088-, 1188-, 1276-, 1351-, 2278-, 2287-, 2334-, and 2464-keV transitions, associated with the decay of the low-spin state in ^{160}Eu, were used to produce the bottom spectrum. (b) Summed background-subtracted time spectrum produced by gating on the 166- and 255-keV transitions in ^{162}Gd, which was used to determine the half-life of the ^{162}Eu high-spin β-decaying state.

from the decay of the low-spin β-decaying state in ^{160}Eu clearly displayed a different half-life. Several such γ rays were summed together to produce the time spectrum also given in Fig. 3(a), from where a value of $T_{1/2} = 30.8\,(5)$ s was determined.

No experimental information was available prior to the present study for the β decay of ^{162}Eu, except for the known half-life that was associated with a single β-decaying state [23]. Similar to ^{160}Eu, two long-lived levels were discovered in ^{162}Eu from the mass measurements. However, only γ rays associated with the decay of the high-spin one were identified in the present study, due to strong contaminations from molecular (^{144}La + H_2O) beam formation in the CARIBU gas catcher. The ground-state band of the ^{162}Gd daughter nuclide was known from prompt fission studies [23] and the in-band γ-ray transitions were used as coincidence gates to isolate structures associated with the β decay of the parent ^{162}Eu nuclide. The strongest β-decay branch is to the 1453-keV level (see Fig. 2), which is tentatively assigned $I^\pi = (6^-)$, based on the proposed configuration, as discussed below. It decays via the 206- and 331-keV γ rays that are visible in the spectrum of Fig. 1(b) to the 1248- and 1122-keV levels, respectively, which are most likely members of the $K^\pi = 2^+$ γ-vibrational band, based on similarities between this structure and the γ band in ^{160}Gd [22]. A time spectrum produced from a summation of individual spectra assembled by gating on the 166- and 255-keV ground-state band transitions is given in Fig. 3(b) from where a half-life of $T_{1/2} = 15.0(5)$ s was determined for the high-spin β-decaying state in ^{162}Eu. Our result differs from the previously reported values of $T_{1/2} = 10.6\,(10)$ s [28] and 11.8 (14) s [29] that were deduced using time spectra produced by gating on the ^{162}Gd x rays and the β particles, respectively. Since the experimental approaches used in Refs. [28,29] to determine the half-life of ^{162}Eu were not able to differentiate between two β-decaying states, these

values may be affected by the decay of the low-spin β-decaying state in ^{162}Eu.

Multiquasiparticle pairing-blocking calculations were carried out using single-particle states based on the Woods-Saxon potential with "universal" parameters [30], deformation parameters β_2, β_4, and β_6 from Ref. [31], and pairing using the Lipkin-Nogami approach [32]. Calculations predict that the most likely configuration for the observed β-decaying states in ^{160}Eu ($N = 97$) is $\pi 5/2[413] \otimes \nu 5/2[523]$. Using the Gallagher-Moszkowski rule [33], $K^\pi = 5^-$ principal quantum numbers can be assigned to the ground state and $K^\pi = 0^-$ to the isomer. Such an interpretation is consistent with the observed decay pattern of two β-decaying states in ^{160}Eu, as well as with the systematics of known proton and neutron orbitals in neighboring nuclei. For example, the $\pi 5/2[413]$ orbital is assigned to the ground state of ^{159}Eu [34], while the $\nu 5/2[523]$ one is associated with the ground state of the $N = 97$, ^{159}Sm and ^{161}Gd, isotones [34,35]. The calculations suggest that the 1999-keV state in ^{160}Gd is associated with the $K^\pi = 5^-$, $\pi^2(5/2[413], 5/2[532])$ configuration. This is supported by the deduced small $\log ft$ value of 5.1 to this level, thus indicating that the parent and daughter configurations are strongly related; they share a common $\pi 5/2[413]$ orbital and the β decay is effectively associated with the $\nu 5/2[523] \rightarrow \pi 5/2[532]$ allowed transition. The proposed configuration for the 1483-keV level is $K^\pi = 4^+$, $\pi^2(5/2[413], 3/2[411])$, and hence, the strong 516-keV γ ray (see Fig. 2) can be interpreted as an allowed $E1$ transition between the $\pi 5/2[532]$ and $\pi 3/2[411]$ orbitals. Further details for these assignments will be discussed in another publication [36].

In ^{162}Eu ($N = 99$), our calculations predict that the neutron Fermi level is located at the $1/2[521]$ neutron orbital and, consequently, the $\pi 5/2[413] \otimes \nu 1/2[521]$ configuration is expected to be lowest in energy, leading to a $K^\pi = 3^-$ and 2^- doublet. Predictions using the Nilsson modified oscillator potential with the universal parameters [37] and the single-particle model based on the folded Yukawa potential [38] lead to identical results. However, such interpretations cannot account for the existence of two long-lived states, as revealed by the mass measurements, and of a high-spin β-decaying state in ^{162}Eu. The next neutron orbital predicted at $N = 101$ is $\nu 7/2[633]$ and, if one raises the position of the $\nu 1/2[521]$ state above the former orbital, then the long-lived levels in ^{162}Eu can be assigned the $\pi 5/2[413] \otimes \nu 7/2[633]$ configuration with $K^\pi = 1^+$ assigned to the ground state and $K^\pi = 6^+$ to the isomer in accordance with the Gallagher-Moszkowski rule [33]. This interpretation is consistent with the observed decay pattern in ^{162}Eu and can explain the observed isomerism in this nucleus. The strong β-decay feeding of the 1453-keV level in ^{162}Gd, coupled with the proposed configuration for the parent state and the predicted two-quasiparticle states in ^{162}Gd, suggests that the $K^\pi = 6^-$, $\nu^2(5/2[523], 7/2[633])$ configuration is most likely associated with this level. It is related to that of the parent state, as they share the same $\nu 7/2[633]$ orbital and the transition is equivalent to the $\pi 5/2[413] \rightarrow \nu 5/2[523]$ decay, which is known to be relatively fast ($\log ft = 6.6$ in ^{159}Eu [34]).

It is striking that three different mean-field potentials fail to describe the correct ordering of single-particle neutron states in the neutron-rich nuclei in this region near $N = 100$. It appears that the single-particle energies are best reproduced when the strength and radius spin-orbit parameters of the Woods-Saxon potential are adjusted, using a fit to the experimentally known states in the $N = 98$ region [39]. However, achieving such an agreement becomes difficult when experimental data are not available. It is also worth noting that deficiencies in the Nilsson model with universal parameters were reported at $N = 100$ in the heavier rare-earth region [40].

While it is always important to properly reproduce the ordering of the single-particle orbitals in order to understand the low-lying spectra, it is worth recognizing in this case that the correct placement of the $1/2[521]$ neutron orbital opens a subshell closure at $N = 98$ with large deformation ($\beta_2 \approx 0.3$) (see, for example, Refs. [37,38,41]). This is in contrast to recent publications suggesting that such a subshell gap exists at $N = 100$ in the neutron-rich nuclei located in the light rare-earth region [12–14].

Additional experimental evidence for the raising of the $1/2[521]$ orbital above the $7/2[633]$ one and for the existence of the $N = 98$ gap can be inferred from several recent studies in the region. For example, $K^\pi = 6^-, \nu^2(5/2[523], 7/2[633])$ and $K^\pi = 4^-, \nu^2(1/2[521], 7/2[633])$ two-quasiparticle isomers were observed in $N = 98$ and 100 nuclei with $Z = 60$, 62, and 64 [42–44]. These indicate that the $\nu 7/2[633]$ orbital precedes the $\nu 1/2[521]$ one, as displayed in Fig. 4. In addition, the energy differences between these two configurations are given in Fig. 4 and it can be seen that the excitation energy of the $K^\pi = 6^-$ state is always 300–500 keV higher than that for the $K^\pi = 4^-$ one. This can be explained by the presence of a large energy gap between the $5/2[523]$ and $7/2[633]$ neutron orbitals at $N = 98$ (see the inset of Fig. 4). It is worth noting the existence of the $N = 98$ deformed subshell gap has already been introduced in studies of other regions of the nuclear chart [45,46]. Hence, the present Letter confirms its presence in the neutron-rich, light rare-earth region.

The existence of a subshell closure also provides a natural explanation for the unexpected observation in the energy of the lowest 2^+ state at $N = 98$ for several even-even nuclei in the light rare-earth region. Figure 5 plots these energies versus neutron number, and a local minimum at $N = 98$ is visible for the dysprosium ($Z = 66$), gadolinium ($Z = 64$), and to a lesser extent, samarium ($Z = 62$) isotopes. Higher deformation is often indicated by lower

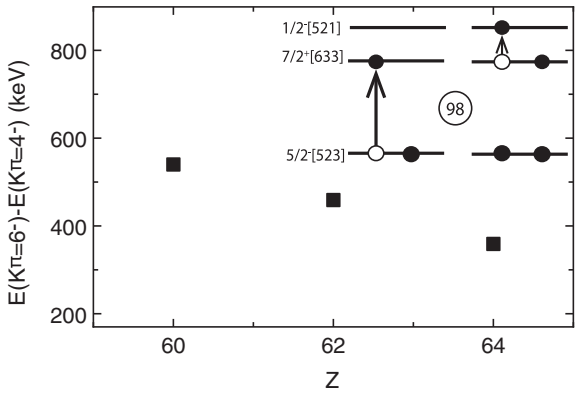

FIG. 4. The solid squares are energy differences between the excitation energies of the $K^\pi = 6^-$, $\nu^2(5/2[523], 7/2[633])$ and $K^\pi = 4^-$, $\nu^2(1/2[521], 7/2[633])$ states in Nd ($Z = 60$), Sm ($Z = 62$), and Gd ($Z = 64$) nuclei at $N = 98$ and $N = 100$, respectively. Data are from Refs. [42–44], as well as from the present Letter for the $K^\pi = 6^-$ state at 1453 keV in ^{162}Gd. (Inset) The single-particle energy level scheme near the neutron Fermi surface for these isotopes.

E_{2^+} values; therefore, Fig. 5 suggests the presence of a localized maximum in deformation at $N = 98$ and near $Z = 64$, which is the midshell for the protons.

In summary, masses, half-lives, and decay properties of multiple β-decaying states were studied in the neutron-rich odd-odd ^{160}Eu and ^{162}Eu nuclei. For the first time, long-lived β-decaying isomers were identified. While multi-quasiparticle blocking calculations using a Woods-Saxon potential with universal parameters correctly predict the properties of the β-decaying states in ^{160}Eu, they fail to describe the observed structure of the ^{162}Eu isotope. It was found that the raising of the $1/2[521]$ neutron orbital above the $7/2[633]$ one is required to explain the decay properties of ^{162}Eu. This also increases the size of the $N = 98$ gap in the single-particle spectrum, which then accounts for the unusual behavior of the first 2^+ level energies for neutron-rich even-even nuclei in the vicinity of the $Z = 64$ midshell in this region.

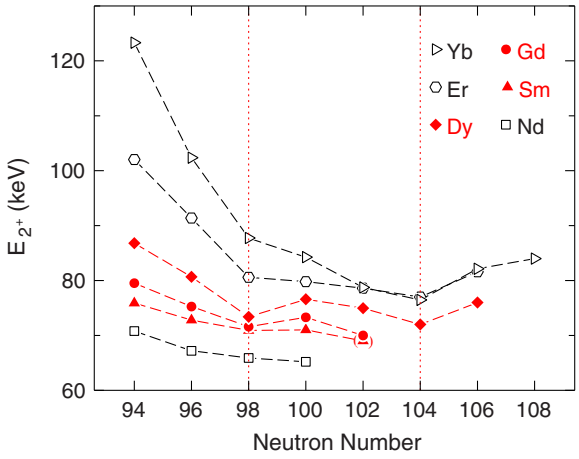

FIG. 5. Energies of the lowest 2^+ states of even-even nuclei in the rare-earth region versus neutron number. Data are taken from the ENSDF database [47].

The authors wish to thank D. C. Radford for his software support. This work is funded by the National Science Foundation under Grant No. PHY-1502092 (USNA) and by the U.S. Department of Energy, Office of Nuclear Physics, under Award No. DE-AC02-06CH11357 (ANL), and NSERC (Canada) under Contract No. SAPPJ-2015-00034 (CPI 1199136). This research used resources of Argonne National Laboratory's ATLAS facility, which is a DOE Office of Science User Facility.

*Present address: Department of Physics, U.S. Naval Academy, Annapolis, Maryland 21402, USA.
†Present address: Universit degli Studi di Milano and INFN, Via Celoria 16, 20133 Milano, Italy.
‡Present address: Department of Physics and Astronomy, University of North Carolina at Chapel Hill, Chapel Hill, North Carolina 27599, USA and Triangle Universities Nuclear Laboratory, Duke University, Durham, North Carolina 27708, USA.

[1] M. G. Mayer, Phys. Rev. **75**, 1969 (1949).
[2] O. Haxel, J. H. D. Jensen, and H. E. Suess, Phys. Rev. **75**, 1766 (1949).
[3] S. G. Nilsson, K. Dan. Vidensk. Selsk. Mat. Fys. Medd. **29**, 16 (1955).
[4] A. Bohr and B. R. Mottelson, *Nuclear Structure* (Addison-Wesley, Reading, MA, 1975), Vol. 2.
[5] R. Surman, J. Engel, J. R. Bennett, and B. S. Meyer, Phys. Rev. Lett. **79**, 1809 (1997).
[6] M. R. Mumpower, G. C. McLaughlin, and R. Surman, Phys. Rev. C **85**, 045801 (2012).
[7] M. R. Mumpower, G. C. McLaughlin, and R. Surman, Phys. Rev. C **86**, 035803 (2012).
[8] M. R. Mumpower, G. C. McLaughlin, R. Surman, and A. W. Steiner, J. Phys. G **44**, 034003 (2017).
[9] M. R. Mumpower, G. C. McLaughlin, and R. Surman, Astrophys. J. **752**, 117 (2012).
[10] M. R. Mumpower, R. Surman, G. C. McLaughlin, and A. Aprahamian, Prog. Part. Nucl. Phys. **86**, 86 (2016).
[11] K. Heyde and J. L. Wood, Rev. Mod. Phys. **83**, 1467 (2011).
[12] L. Satpathy and S. K. Patra, J. Phys. G **30**, 771 (2004).
[13] S. K. Ghorui, B. B. Sahu, C. R. Praharaj, and S. K. Patra, Phys. Rev. C **85**, 064327 (2012).
[14] Z. Patel *et al.*, Phys. Rev. Lett. **113**, 262502 (2014).
[15] G. Savard, S. Baker, C. Davids, A. Levand, E. Moore, R. Pardo, R. Vondrasek, B. Zabransky, and G. Zinkann, Nucl. Instrum. Methods Phys. Res., Sect. B **266**, 4086 (2008).
[16] T. Hirsh *et al.*, Nucl. Instrum. Methods Phys. Res., Sect. B **376**, 229 (2016).
[17] J. Van Schelt *et al.*, Phys. Rev. Lett. **111**, 061102 (2013).
[18] S. Eliseev, K. Blaum, M. Block, C. Droese, M. Goncharov, E. M. Ramirez, D. A. Nesterenko, Y. N. Novikov, and L. Schweikhard, Phys. Rev. Lett. **110**, 082501 (2013).

[19] S. Eliseev *et al.*, Appl. Phys. B **114**, 107 (2014).
[20] M. Wang, G. Audi, F. G. Kondev, W. J. Huang, S. Naimi, and X. Xu, Chin. Phys. C **41**, 030003 (2017).
[21] A. J. Mitchell *et al.*, Nucl. Instrum. Methods Phys. Res., Sect. A **763**, 232 (2014).
[22] C. W. Reich, Nucl. Data Sheets **105**, 557 (2005).
[23] C. W. Reich, Nucl. Data Sheets **108**, 1807 (2007).
[24] N. A. Morcos, W. D. James, D. E. Adams, and P. K. Kuroda, J. Inorg. Nucl. Chem. **35**, 3659 (1973).
[25] J. M. D'Auria, R. D. Guy, and S. C. Gujrathi, Can. J. Phys. **51**, 686 (1973).
[26] J. D. Baker, R. J. Gehrke, R. C. Greenwood, and D. H. Meikrantz, J. Radioanal. Chem. **74**, 117 (1982).
[27] H. Mach, A. Piotrowski, R. L. Gill, R. F. Casten, and D. D. Warner, Phys. Rev. Lett. **56**, 1547 (1986).
[28] R. C. Greenwood, R. A. Anderl, J. D. Cole, and H. Willmes, Phys. Rev. C **35**, 1965(R) (1987).
[29] J. Wu *et al.*, Phys. Rev. Lett. **118**, 072701 (2017).
[30] S. Cwiok, J. Dudek, W. Nazarewicz, J. Skalski, and T. Werner, Comput. Phys. Commun. **46**, 379 (1987).
[31] P. Möller, A. J. Sierk, T. Ichikawa, and H. Sagawa, At. Data Nucl. Data Tables **109–110**, 1 (2016).
[32] W. Nazarewicz, J. Dudek, R. Bengtsson, T. Bengsson, and I. Ragnarsson, Nucl. Phys. **A435**, 397 (1985).
[33] C. J. Gallagher, Jr. and S. A. Moszkowski, Phys. Rev. **111**, 1282 (1958).
[34] C. W. Reich, Nucl. Data Sheets **113**, 157 (2012).
[35] C. W. Reich, Nucl. Data Sheets **112**, 2497 (2011).
[36] D. J. Hartley *et al.* (unpublished).
[37] R. Bengtsson and I. Ragnarsson, Nucl. Phys. **A436**, 14 (1985).
[38] P. Möller, J. R. Nix, and K. L. Kratz, At. Data Nucl. Data Tables **66**, 131 (1997).
[39] J. Dudek and T. Werner, J. Phys. G **4**, 1543 (1978).
[40] F. G. Kondev, G. D. Dracoulis, A. P. Byrne, T. Kibedi, and S. Bayer, Nucl. Phys. **A617**, 91 (1997).
[41] F. G. Kondev, G. D. Dracoulis, and T. Kibédi, At. Data Nucl. Data Tables **103–104**, 50 (2015).
[42] R. Yokoyama *et al.*, Phys. Rev. C **95**, 034313 (2017).
[43] E. Ideguchi *et al.*, Phys. Rev. C **94**, 064322 (2016).
[44] Z. Patel *et al.*, Phys. Lett. B **753**, 182 (2016).
[45] D. G. Burke and G. Løvhøiden, Nucl. Phys. **A750**, 185 (2005).
[46] H. J. Jensen *et al.*, Z. Phys. A **359**, 127 (1997).
[47] www.nndc.bnl.gov/ensdf.